



ELSEVIER

Contents lists available at ScienceDirect

Computer Networks

journal homepage: www.elsevier.com/locate/comnetDynamic system model for optimal configuration of mobile RFID systems [☆]Juan J. Alcaraz ^{*}, Esteban Egea-López, Javier Vales-Alonso, Joan García-Haro

Department of Information Technologies and Communications, Technical University of Cartagena (UPCT), Plaza del Hospital 1, 30202 Cartagena, Spain

ARTICLE INFO

Article history:

Received 8 January 2010

Received in revised form 25 June 2010

Accepted 28 July 2010

Available online xxx

Keywords:

Radio frequency identification

Frame slotted ALOHA

Equilibrium point analysis

Stability

Discrete time system

Tag loss ratio

ABSTRACT

In many practical RFID applications tags are attached to items that pass through the reader's field moving at a constant speed, following a fixed path. The time-constrained presence of the tags in the identification region introduce the possibility that tags exit the system without being identified (*lost* tags). Reliability is a practical requirement in most applications, which implies that the portion of lost tags should be kept below a very small threshold. Therefore, we take this fact as the starting point in the design process. We present a mathematical model for RFID systems implementing Frame Slotted Aloha as the collision resolution protocol. Upon this model it is possible to compute the tag loss ratio and therefore to obtain the optimal frame size in terms of reliability. While previous works generally use a Markovian approach, our model is based on dynamic systems theory, having a smaller computational cost which, in addition, is independent of the dimension of the system. Moreover, the proposed model allows us to identify the multiplicity of the equilibrium points in the system, an interesting and relevant property that has been overlooked in RFID systems so far. Finally, we present a design procedure based on our model that allows to configure the physical parameters of the system in order to adjust both the throughput and the reliability.

© 2010 Published by Elsevier B.V.

1. Introduction

The automatic identification of objects plays a central role in many industrial, logistical and commercial activities such as inventory management, supply chain automation, electronic toll collection, anti-theft systems and access control. Radio frequency identification (RFID) is an increasingly deployed technology that allows tagged objects to be uniquely identified by means of near/far-field wireless communications. Although RFID is a more expensive technology than bar-code reading, it comprises many advantages compared to it, namely its higher data holding capacity

and the fact that it enables remote identification which, depending on the transmission frequency, makes RFID tagged objects identifiable within up to 3 meters distance [1].

An RFID system comprises two basic components: RFID tags (transponders) and RFID readers (transceivers). A tag consists of a microchip with an embedded antenna and a small memory that stores a unique identifier, the Electronic Product Code (EPC), providing an unambiguous numbering scheme that allows any object to be identified worldwide. In typical RFID applications, tags are attached to items of interest so that the host items can be effectively monitored by the system using tag readers. When tags are interrogated by a reader, they respond with their EPC. We focus on applications using passive RFID tags which, in contrast to active ones, do not hold an internal power source such as a battery. Instead, they obtain the energy from an electromagnetic signal transmitted by the reader. Tags within the interrogation zone of a reader can absorb the energy from this signal by means of inductive coupling.

[☆] This work was supported by project grants TEC2007-67966-01/TCM (CON-PARTE-1) and CALM TEC2010-21405-C02-02 and it was also developed in the framework of "Programa de Ayudas a Grupos de Excelencia de la Región de Murcia, Fundación Seneca".

^{*} Corresponding author. Tel.: +34 968 32 65 44.

E-mail addresses: juan.alcaraz@upct.es (J.J. Alcaraz), esteban.egea@upct.es (E. Egea-López), javier.vales@upct.es (J. Vales-Alonso), joang.haro@upct.es (J. García-Haro).

The received energy is converted into electrical current and stored in an on-board capacitor so that it can be used for the subsequent transmission of the EPC in response to the reader interrogation signal [2].

Each reader can only interrogate tags within its vicinity or interrogation region, [3], where the reader's electromagnetic field is strong enough to energize the tags. This region is also referred to as reader's field or coverage area [4]. When multiple tags receive the interrogation signal, there is a chance that more than one tag reply simultaneously. Multiple responses at the same time on the radio communication channel reduces the signal to noise ratio at the reader's receiver which usually implies that the reader cannot decode the data contained in the reply signals. This event is called tag collision and is the main reason of the decrease of efficiency in RFID systems. How to effectively solve this problem is one of the critical research issues in practical RFID applications, [5].

Several collision resolution protocols have been proposed so far. They can be broadly classified into two groups: deterministic and probabilistic. Among them, Framed Slotted ALOHA (FSA), a probabilistic one, is the most usual in RFID standards and commercial products, ISO/IEC-18000-6C [6] and EPCglobal UHF Generation 2 RFID [7]. In a general FSA-based system, the reader starts an identification cycle (frame) by broadcasting a message including the number of identification opportunities (time-slots). After receiving this message, each tag under coverage randomly selects one of the slots to reply with its EPC. A collision takes place when more than one tag response in the same slot. A slot is said to be successful if only one tag responses in this slot and its message is correctly decoded by the reader. If the protocol supports muting, the tags whose reply is acknowledged by the reader withdraw themselves from contention in subsequent identification cycles. In the non-muting version of FSA, tags contend either if they have been previously identified or not, since the reader do not send acknowledgment messages to identified tags.

If the number of slots in a frame (frame length or frame size) remains static during system operation, the protocol is referred to as Basic FSA (BFSA). When the frame length is variable, it is called Dynamic FSA (DFSA). The frame size has a strong influence on the performance of RFID systems and has been subject of study of several previous works, [2,3,8]. Depending on the number of tags under coverage, a small frame size increases the probability of collision while a large frame size may be inefficient. Therefore, most of the previous works has focused on how to dynamically adapt the frame length to improve the identification process performance in terms of number of identified tags per second.

Very frequent practical scenarios involve tags attached to moving objects [4,9–11], that is, tags arrive and leave the coverage area after some time. Since there is a limited time for the reader to identify the passing tags, it is critical to determine not only how fast the identification process is (the common performance metric) but also how many tags leave the coverage area without being identified, that is, the reliability of the process. In this case, frame sizing is a more challenging problem than in static tag scenarios

since the frame size is also related to the number of tags entering at each identification cycle and to the number of cycles that each tag could participate in.

Systems involving moving tags are generally referred to as mobile RFID systems [4,12–14]. A typical example of them would be a reader installed at the dock door of a warehouse facility to retrieve the codes from incoming and outgoing items. Such a portal would be equipped with RFID readers to identify passing tags and automatically update the central database with the captured information [15]. Another typical example is a conveyor belt in an factory or a logistic center where pallets, cases and objects attached with RFID tags have to be tracked. In these situations, tags generally move along a fixed path at a constant speed. Fig. 1 conceptualizes this scenario and depicts some of its main parameters: the length of the reader's coverage area, the velocity (assumed constant) of the tag flow and the number of identification cycles that tags may participate in during their time within the interrogation region.

In this work we address the parameter configuration of mobile RFID systems. Throughput and reliability are two main concerns of the design process. Throughput refers to the number of tags identified per unit of time and reliability refers to the probability of a tag exiting the interrogation region without successfully transmitting its EPC. We will refer to such a tag as a *lost* tag. Therefore we will measure the reliability in terms of tag loss ratio (TLR), defined as the quotient between the number of lost tags and the total number of tags entering the interrogation region.

Intuitively, one may think that the frame length, the speed and the density of the tag stream (in tags per unit of distance) are related to both the throughput and the reliability of the system. Moreover, it is reasonable to expect a trade-off between the TLR and the number of tags entering the reader's field per unit of time. In this paper we propose a simple mathematical model that allows us to compute the TLR from the aforementioned system parameters for a BFSA-based system implementing the muting feature. This model is used to obtain the frame length minimizing the TLR. The TLR obtained is validated by simulations and compared with a reference DFSA algorithm. The proposed procedure also allows us to generate the set of speed-tag

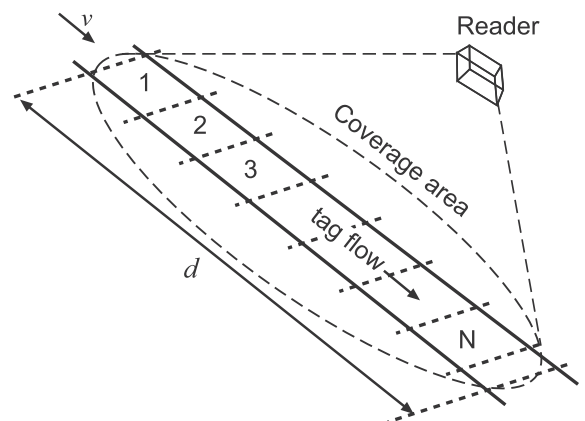


Fig. 1. System diagram.

density combinations for which the system can operate under a given TLR objective, illustrating the concept of operative region which summarizes the relationship between the system parameters and the trade-offs between them. The computation of the operative region has very interesting practical implications, e.g. it let us determine how fast a vehicle whose load must be identified can pass in front of an RFID reader or how many identifiable objects can be transported on a conveyor belt moving at a given speed.

One innovative aspect of our model is that it does not rely on Markovian modeling, which has been the typical analytical tool for the performance analysis of ALOHA-based systems. Instead, we base our analysis on dynamic systems theory formulation. As we discuss in the following section, the main drawback of applying the classical Markov approach to our scenario is that, as the dimension of the problem increases (e.g. the number of tags in the interrogation region or the number of identification cycles during the sojourn time) the model becomes computationally cumbersome. In contrast, the dynamic system formulation not only allows a fast computation of the TLR, but it is also insensitive to the dimension of the problem.

Moreover, the proposed model let us disclose interesting and relevant properties of the system. We show that, at certain configurations, a system operating at a desirable TLR may eventually switch to a much higher and completely unacceptable TLR. Why does this happen? The analysis of the dynamic system equation reveals that, in some cases, the system has multiple equilibrium points, each one associated to different TLR values. Therefore, it would be safer for most applications to opt for configurations with only one equilibrium point. The multiplicity of equilibrium points is a well-known issue in classical slotted ALOHA systems [16,17] where it was studied in the framework of Markov analysis for systems with a constant number of stations and Poisson traffic. It is interesting to see that this feature is also present in a mobile RFID scenario, where the use of FSA and the fact that tags are mobile are substantial differences with respect to the ALOHA systems where this characteristic was found.

In the following section we discuss the related work and highlight what are the contributions of our paper in contrast to previous ones. In Section 3 the model is presented. Based on this model, we discuss in Section 4 the multiplicity and stability of the equilibrium points of the system. In Section 5, the model is validated and evaluated by simulation. Finally, in Section 6 the operative regions are shown before concluding in Section 7.

2. Related work

The performance in terms of delay and throughput of ALOHA systems has been extensively analyzed in the past mainly by using Markov chain models. Kleinrock [18, pp. 360–393] provides a classical review. C. Wang, et al. develop in [21] a Discrete Time Markov Chain model for the EPC-global UHF (Gen-2) RFID protocol with adaptive frame length (DFSA). However, in a mobile tag scenario the departure instant is closely related to the metric of inter-

est, the TLR, and therefore some information about the position of the tags has to be introduced in the model, increasing the number of states and making the procedure computationally cumbersome even without the dynamic frame length adjustment scheme. This problem has been sometimes referred to as the *curse of dimensionality*. We already stated this fact in our previous works [10,22], where we developed a Markovian model for this type of system. The model, although useful for validation and benchmarking purposes, was only practical for a relatively small number of incoming tags and identification slots.

The stability and multiplicity of the equilibrium points in ALOHA systems have been shown and studied in [16,17] by using the concept of expected drift in the framework of Markov modeling. The expected drift provides the expected direction of movement of the system over the state space during a random walk. At an equilibrium point the drift is near to zero, and the point is said to be stable if the drift of the states at its vicinity is directed to the equilibrium point. This essentially means that if the system is near a stable equilibrium point, it will remain at nearby states for a long time. It was shown that ALOHA systems may have either one or two stable equilibrium points. In the latter case, the throughput of one point (the *desirable* one) is larger than the other (*undesirable*) one. As we will see, in our case, when the system operates at an undesirable equilibrium point, the tag loss ratio is extremely high rendering the system useless for identification purposes. Our goal is obtaining a frame length value that minimizes the TLR or, more generally, to find the configuration that assures that the system always operates under a given performance objective. Therefore, the most reliable policy is to avoid configurations with multiple equilibrium points even though one of them presents an acceptable TLR, since there is always the chance that the system falls in the undesirable point causing the loss of lots of tags. Our model allows a simple and intuitive graphical analysis of the equilibrium points and their stability.

Most previous works on FSA protocols for RFID focus on DFSA, where the main goal is to find good estimates of the population of unidentified tags under coverage based on the feedback provided by the outcome of the identification cycle. The goal in these works is to dynamically adapt the frame length to the estimated number of tags in order to optimize the desired performance objective. As representative examples, Floerkemeier [19] uses a Bayesian estimation whereas Chen [20] uses a maximum likelihood estimation. Fewer works address the optimization of the frame length in a BFSA scenario. Z.G. Prodanoff offers in [2] an analytical solution of the optimal frame size in the non-muting version of BFSA, for a non-mobile RFID system.

The mobile RFID scenario has been addressed in [12,11] from the point of view of physical parameters for electronic design (antenna angle, signal strength, electromagnetic induction, etc.) that are out of the scope of our work. Other works like [3,4,13,14] focus on the frame sizing problem in mobile RFID scenarios, highlighting its importance in practical applications. All these works propose modifications to DFSA following the main trend of adapting the frame size at the beginning of each identification cycle according to the estimation of the number of

unidentified tags obtained in previous cycle. Note that this procedure implies two requirements to the system: first, that DFSA is implemented and second, that the tag estimation algorithm is fast enough to compute the tag population estimate within the time gap between two identification cycles. Our model is applicable to the simpler and widely deployed BFSAs-based systems. Nevertheless, in order to assess its performance, we use as benchmark a DFSA protocol with a *perfect* tag population estimator, i.e. the RFID reader knows the tag population at the beginning of each identification cycle and selects the frame length that minimizes the TLR.

Summarizing, our work differs from previous ones in three main aspects: first, we focus on a mobile RFID scenario but, in contrast to previous works, we consider a BFSAs system with muting feature instead of DFSA. Second, while previous works mainly focus on finding the frame size that maximizes the throughput, we adopt a broader view that also addresses the configuration of physical parameters (velocity, coverage area, etc.) and gives more importance to reliability as required by practical applications. Third, we develop a model based on dynamic system theory, which is a novel approach for the performance analysis of RFID systems. This formulation overcomes the limitations of the Markovian approach for the dense mobile RFID scenario. This is our first contribution and the basis upon which we accomplish the following ones:

- We disclose the multiplicity of stable points in mobile RFID systems and discuss its theoretical interest and practical implications.
- We compare the optimized BFSAs with an *ideal* DFSA with perfect knowledge of the tag population, showing that, in a mobile tag scenario, their performances are identical in terms of TLR.
- We show that, when configuring the physical parameters of the system, a tradeoff between throughput and performance arises.
- We introduce the concept of operative region providing a simple but useful design procedure for practical mobile RFID systems.

3. System model

In this section we analyze the operation of an RFID system with moving tags implementing the EPCglobal Gen-2 FSA anti-collision procedure [7], which follows the general FSA scheme but has the particularity that the durations of idle and successful/collision slots are different, since the muting feature considered implies that the reader acknowledges identified tags. Because we are considering BFSAs, the number of identification slots of the FSA frame (frame length) is constant during the operation of the system.

The operation is as follows: the reader issues a *Query* packet containing the Q parameter $[0, \dots, 15]$ that sets the number of identification slots in the subsequent FSA frame to 2^Q . The tags that have received the *Query* command select randomly a slot number between $[0, 2^Q - 1]$ and load it onto their slot counter. Each tag decrements its slot counter upon receiving a *QueryRep* command from

the reader and transmits a response packet with a 16-bit random number when the counter reaches zero. At each identification slot, 0, 1 or more tags may send a response packet, resulting in an idle, successful or collision slot respectively. After a successful slot, the reader sends an *Ack* packet that reserves an exclusive time slot where the successful tag transmits its electronic product code (EPC). In consequence the duration of successful slots (T_s) is longer than the duration of idle and collision slots (T_u).

Fig. 1 depicts the system: tags pass through the coverage area at a constant speed v , as in [4,14]. The tag flow is also characterized by the tag density, δ (given in tags/m) in the direction of tag motion. Note that v and δ are related to the tag arrival rate, which is a parameter used in other works. The coverage area has a length d in this direction. Note that δ may denote an average value since the number of tags per length unit may be a random variable. The system model is based on formulating the relationships among the average values of the system variables.

Let p denote the average number of unidentified tags in the reader's coverage area. In the following we will also refer to this quantity as the tag *population*. It is assumed that a tag can only be identified in a frame if it remains under coverage during the whole duration of the frame. The simulation results in Section 5 show that this assumption implies an overestimation of the TLR in scenarios where tags stay under coverage for a very small number of frames. In consequence, the model follows a worst-case strategy which is appropriate for the applications considered. The frame length is denoted by $L = 2^Q$. A tag moving at a constant speed, v , remains under coverage for a limited amount of time. During this time, each tag will participate in, at most, N full identification cycles (frames).

$$N = \left\lfloor \frac{d}{TLv} \right\rfloor, \quad (1)$$

where T denotes the average slot duration. The coverage area can be divided into N segments, corresponding to the N frame periods that each tag spends in the system, as shown in Fig. 1. The number of unidentified tags at the n -th segment is a stochastic process whose average value, in steady state, is p_n . It is clear that

$$\sum_{n=1}^N p_n = p, \quad (2)$$

Fig. 2 shows an example of the average number of unidentified tags per segment. In the last segment, only a portion of tags (α) will participate in the upcoming identification cycle. This portion is given by:

$$\alpha = \frac{d}{TLv} - N. \quad (3)$$

The framed operation of FSA implies the following system dynamics. At each identification cycle, (i) δTLv new tags enter segment 1, (ii) the tags in segment n move to segment $n + 1$ for $n = 1, \dots, N - 1$ and (iii) the tags in segment N exit the coverage area. The first fact is formulated as

$$p_1 = \delta TLv. \quad (4)$$

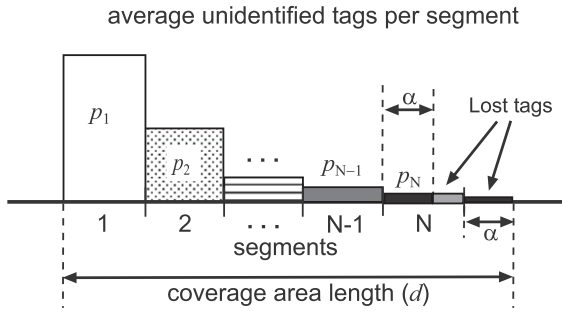


Fig. 2. Example of the unidentified tags distribution along the coverage area.

Let us remark here that p_1 represents the average number of tags entering the first stage, therefore we can apply this model to random arrival processes just by substituting the right hand side of (4) with the expected value of the arrivals. Given an average number p of unidentified tags, let I denote the average number of identified tags per frame. Assuming that every tag under coverage has the same success probability, the average number of tags identified in segment n is determined by the proportion of unidentified tags in this segment, i.e. it is given by $I p_n/p$. Then, according to the system dynamics, p_{n+1} equals the average number of unidentified tags in previous segment, p_n , minus the identified ones, $I p_n/p$. This fact is expressed by the following set of equations

$$p_{n+1} = p_n(1 - I/p), \quad \text{for } n = 1, \dots, N - 2. \quad (5)$$

In the last segment, only a portion α of the incoming tags participate in the identification process. Thus, its associated equation is:

$$p_N = \alpha p_{N-1}(1 - I/p). \quad (6)$$

There are two particular cases where previous equations do not hold. First, if $N = 1$ tags enter directly into the last segment. The average number of unidentified tags is then given by a single equation

$$p = \alpha \delta TLv. \quad (7)$$

Second, if $N = 0$, tags do not stay long enough to be identified and therefore, $p = 0$. If we assume that the duration of every slot is equal to T_u , the frame length is constant and equal to $T_u(L + 1)$, including the initial tag activation slot of the frame. However, as explained previously, the duration of a successful slot is longer ($T_s > T_u$). Therefore, T is given by

$$T = \frac{T_u(L + 1) + I(T_s - T_u)}{L}. \quad (8)$$

Assuming that no capture effect is present, i.e. a successful ID reading occurs only when exactly one tag transmits its ID during a slot, the average number of identified tags at each FSA identification cycle, I , is approximated by

$$I \approx p \left(\frac{L - 1}{L} \right)^{p-1}, \quad (9)$$

where the function in the right side provides the expected number of identifications given a number of tags in an FSA system [23]. In our case, this expression is approximate

since p is the average population. In the simulations performed in order to validate the model it was found that this approximation has no effect on the accuracy of the model, especially in terms of TLR measurement.

Applying the normalization condition (2), the system of equations given by (4)–(6) is reduced to the following equation

$$\delta TLv \left(\sum_{n=0}^{N-2} \left(1 - \frac{I}{p} \right)^n + \alpha \left(1 - \frac{I}{p} \right)^{N-1} \right) = p, \quad (10)$$

where N , α , T and I are given by (1), (3), (8) and (9) respectively. Note that all previous variables depend on p . Therefore, although it is not explicitly stated for the sake of clarity, the right notation for each one is $N(p)$, $\alpha(p)$, $T(p)$ and $I(p)$.

Eq. (10) can be numerically solved to obtain p within the set of feasible values: $\delta d \geq p \geq \delta TLv$. Then, from the system of Eq. (5) we can obtain p_i for $i = 1, \dots, N$ as a previous step for the computation of the TLR. However, before addressing this issue, it is convenient to study the solutions of Eq. (10) which, as next section shows, provides a useful insight into the properties of the system.

4. Equilibrium points

We are now interested in the equilibrium points of the system defined by the solutions of Eq. (10). It is well-known that a slotted ALOHA system with fixed population and random transmission attempts can have either one or two stable equilibrium points [17]. In this section we show that this property is also present in a BFSA-based mobile RFID system. Therefore we can determine, for each Q , whether the solution obtained corresponds to a desirable or an undesirable equilibrium point. The classical approach consists on studying the expected drift of the system [17], that is, the expected distance between the current state and the following state. The expected drift is obtained in the framework of Markov modeling and therefore it suffers from the previously mentioned *curse of dimensionality*, since it requires the computation of every transition probability in the state space in order to perform a conditional expectation operation at each state. In our model, the study of the equilibrium points is based on the stability analysis of dynamical systems [24]. The computational complexity of the associated procedure is negligible independently of the dimension of the state space.

Let us consider the nonlinear, discrete dynamical system governed by Eq. (10), and let p_t denote the value of the state variable of this one-dimensional, deterministic system at time t . The evolution of the state variable over time is determined by

$$p_{t+1} = f(p_t), \quad t = 0, 1, 2, \dots, \quad (11)$$

where $f(p_t)$ is the left hand side of Eq. (10) with the argument p_t instead of p . Note that (11) does not really provide the number of unidentified tags over time, since the real system operates under random conditions that are not considered in this equation. As $t \rightarrow \infty$, the state variable converges to a steady state equilibrium \bar{p} , such that $\bar{p} = f(\bar{p})$. If the system has multiple steady state equilibrium points,

the stability properties of each one and the initial state p_0 determine where the system tends to converge. Note that the equilibrium points coincide with the solutions of (10).

Since the state variable is one-dimensional, we can study the equilibrium points and their stability graphically. Let us consider a reference scenario where tags enter the coverage area at a speed $v = 1$ m/s, the density of tags is $\delta = 80$ tags/m, the length of the coverage area is $d = 2$ m and the durations of a successful and an unsuccessful slot are $T_s = 4$ ms and $T_u = 2$ ms respectively.

Fig. 3 illustrates the graphical analysis of the associated dynamical system in the reference scenario with $Q = 4$. In this figure, the points where the graph of $p_{t+1} = f(p_t)$ intersects the line $p_{t+1} = p_t$ are the equilibrium points. Let $p_{t+1} = a p_t + b$ be a linear approximation of $f(p_t)$ in the neighborhood of an equilibrium point. A well-known result of dynamical system theory [24] is that if $|a| < 1$, then the equilibrium is locally stable whereas if $|a| > 1$ then the equilibrium is unstable. Consequently, it is clear that \bar{p}_1 and \bar{p}_3 in Fig. 3 are locally stable while \bar{p}_2 is unstable. Moreover, the graph suggests that the state variable will converge to \bar{p}_1 if $p_0 < \bar{p}_2$ and to \bar{p}_3 if $p_0 > \bar{p}_2$. This fact has relevant consequences in the real system, which can operate either at $p = \bar{p}_1$ or at $p = \bar{p}_3$, i.e., the number of unidentified tags under coverage may oscillate around two possible equilibrium points. While the former p value may be adequate, the latter is associated to a high TLR, which is unacceptable for RFID applications.

In order to assess the correspondence of the graphical analysis with the behavior of the real system we have simulated the reference scenario for several initial populations of unidentified tags, generating a set of traces with the evolution of this parameter. Fig. 4 depicts the set of traces for a system configured to $Q = 4$. For the sake of clarity, the points in the curves have been exponentially averaged, reducing the variability caused by the randomness of the process. It can be checked that, depending on the initial state, the system tends to oscillate, after a transient period, around two possible values of p that correspond to the stable equilibrium points identified in Fig. 3. Obviously, due to the stochastic nature of the system, the initial configura-

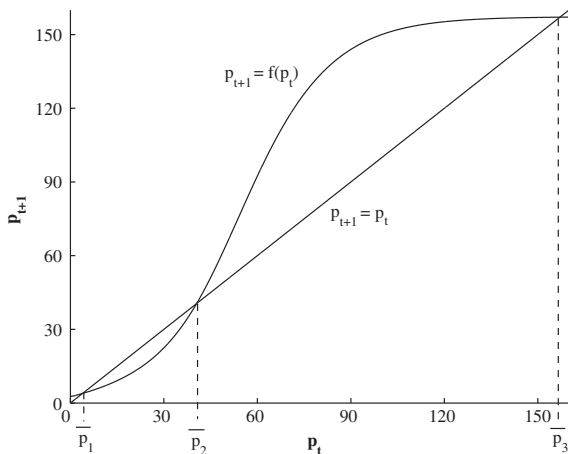


Fig. 3. Graphical analysis of the associated dynamical system for the reference scenario with $Q = 4$.

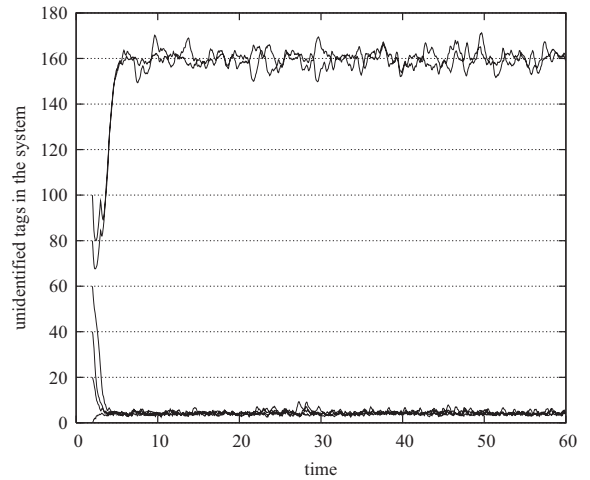


Fig. 4. Simulated evolution of the number of unidentified tags for several initial populations in the reference scenario with $Q = 4$.

tion that causes the system to operate at an undesirable p is not exactly determined by the unstable state \bar{p}_2 , although this value gives a rough idea about what is the number of unidentified tags that causes the system to operate at an undesirable state.

Let us now consider the reference scenario configured to $Q = 5$. In this case the graphical analysis is illustrated in Fig. 5. In contrast to previous Q setting, now there is only one steady state equilibrium which, according to previous considerations, is globally stable. The implications of this fact in the real system can be observed in the simulation-based traces depicted in Fig. 6. When $Q = 5$ the system always converges to a single p value, independently of the initial configuration. This desirable property implies that the system is capable to recover from eventual saturation of collision events (e.g. because of a temporal and abrupt increase of the tag density), at least within the range of operation parameters.

The main conclusion drawn from this section is that, like all the ALOHA-based systems, the BFSMA system with mobile

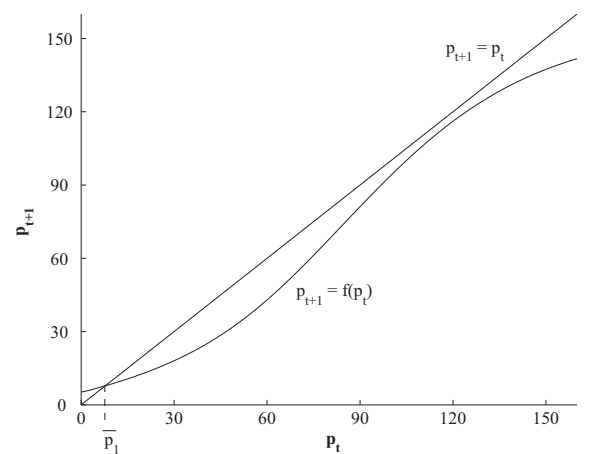


Fig. 5. Graphical analysis of the associated dynamical system for the reference scenario with $Q = 5$.

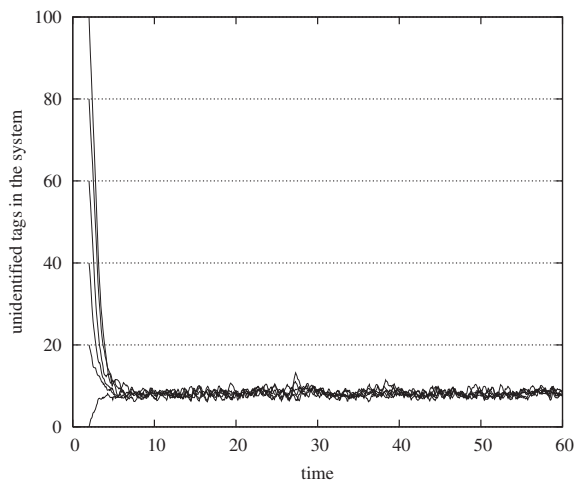


Fig. 6. Simulated evolution of the number of unidentified tags for several initial populations in the reference scenario with $Q = 5$.

tags may converge to more than one average population of unidentified tags, which means that even a system that performs correctly most of the time may eventually switch to an undesirable operation state. Therefore, following the worst-case approach required by an RFID application, in the following sections we always consider the largest solution of Eq. (10) for the computation of the TLR.

5. Performance evaluation

The (average) number of lost tags per identification cycle, denoted by l , is given by the average amount of tags that leave segment N without being identified. As shown in Fig. 2, two quantities contribute to l : The tags entering the part of segment N where they cannot stay for a whole frame, $(1 - \alpha)p_{N-1}(1 - l/p)$, and the tags in segment N that fail to identify, $p_N(1 - l/p)$. Adding both contributions we obtain

$$l = ((1 - \alpha)p_{N-1} + p_N) \left(1 - \frac{l}{p}\right). \quad (12)$$

In the particular case of $N = 1$, l is given by

$$l = (1 - \alpha)\delta TLv + p - l. \quad (13)$$

Finally, if $N = 0$, then $l = \delta TLv$. The TLR is obtained by dividing l by the number of incoming tags per frame

$$TLR = \frac{l}{\delta TLv}. \quad (14)$$

The mathematical model presented in this paper was validated by comparing the TLR obtained numerically with the TLR measured in simulations. The simulator was specifically developed for the systems considered in this paper (mobile RFID with BFSA or DFSA anti-collision protocols) and is based on the discrete-event simulation methodology. The simulation runs last until the confidence interval of each TLR obtained is less than 0.5% with a confidence degree of 95% according to a t-student distribution. In the simulations, the number of tags entering the system each identification cycle is a random value because, even

though the linear density is fixed, the position of the tags in the line is random. Fig. 7 compares both sets of results showing, for several δ values, the TLR versus the Q factor in the reference scenario ($d = 2$ m, $T_u = 2 \cdot 10^{-3}$ s, $T_s = 4 \cdot 10^{-3}$ s and $v = 1$ m/s). We can also observe the minimum TLR for each δ . As expected, the mathematical model provides an upper bound for TLR at values of Q associated to a small N while, in general, the tendency is accurately described, especially for optimal configuration purposes.

These figures also provide an interesting example of the tradeoff between throughput and reliability in a mobile RFID system. Maximizing the throughput, defined as the number of tags identified per second, is the main objective in most works addressing frame length optimization in RFID. However, the figure shows that when the incoming tag flow is $v\delta = 80$ tags/s, the best achievable throughput equals the incoming flow and is obtained when the TLR is very close to zero. In contrast, for $v\delta = 150$ tags/s, the maximum throughput is 133.9 tags/s, obtained at $Q = 7$ where the TLR is minimum and equal to 11%. When $v\delta = 200$ tags/s, the minimum TLR, obtained with $Q = 8$, is 33%, and therefore the maximum throughput at this flow is 134 tags/s. These results suggest that, when configuring the tag density and velocity (*i.e.* the tag flow), increasing the throughput implies decreasing the reliability of the identification process.

In order to illustrate this tradeoff, Fig. 8 contrasts the minimum achievable TLRs with their associated (maximum) throughputs for a wide range of incoming tag flows, given in tags per second. Each set of values is obtained for three different velocities of the tag movement, showing that it is the velocity–density product (tag flow) what

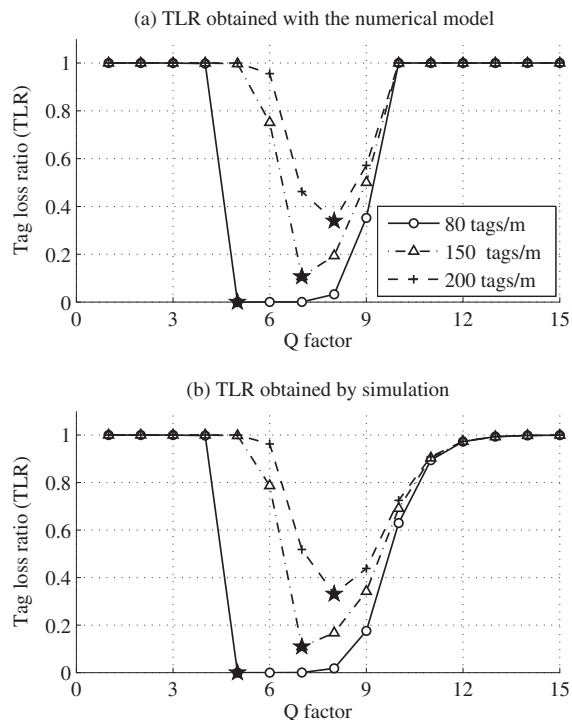


Fig. 7. Tag loss ratio versus Q for several tag densities.

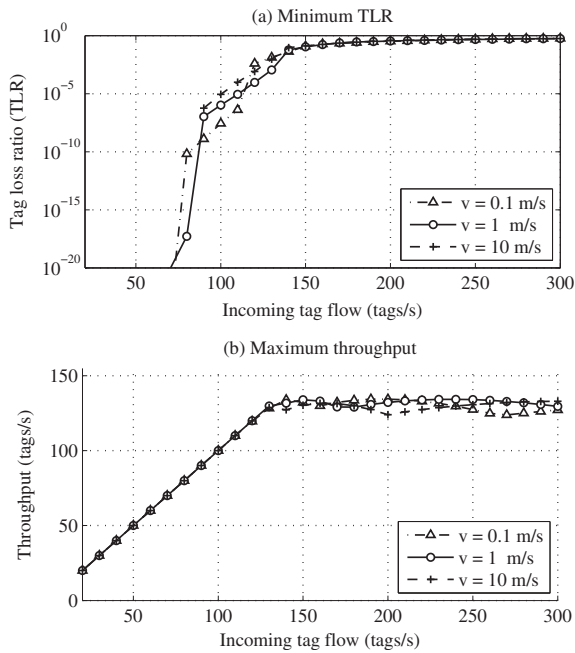


Fig. 8. Minimum TLR and maximum throughput versus the incoming tag flow.

mainly determines the performance. It is clear from these figures that the design procedure for a practical RFID system with mobile tags should start by fixing the desired TLR objective and then determining the set of parameters for which this TLR can be achieved, *i.e.* the system should operate at a parameter setting such that the TLR obtained with the optimum Q is smaller than the objective TLR. The following section focuses on this procedure.

In a Q -static system, the optimum Q can be computed offline with the procedure described. Nevertheless, because of the relatively small amount of allowed Q values $[0, \dots, 15]$, the procedure is fast enough for an online re-computation in systems that can detect changes in some parameters. For instance, a weight sensor associated to the load area of a conveyor belt may allow the reader to in-

Table 1
Optimum Q for an ideal dynamic Q system

Optimum Q	p range
0	$p = 1$
1	$1 < p \leq 3$
2	$3 < p \leq 6$
3	$6 < p \leq 11$
4	$11 < p \leq 22$
5	$22 < p \leq 44$
6	$44 < p \leq 89$
7	$89 < p \leq 177$
8	$177 < p \leq 355$
9	$355 < p \leq 710$
10	$710 < p \leq 1420$
11	$1420 < p \leq 2839$
12	$2839 < p \leq 5678$
13	$5678 < p \leq 11357$
14	$11357 < p \leq 22713$
15	$p > 22713$

fer the tag density and thus to recompute the optimum Q accordingly. The average number of fixed-point iterations required to compute p for the three δ values of Fig. 7 (a) (80, 150 and 200 tags/m) are 7.3, 6.7 and 4.6 respectively.

Finally, it is worth obtaining the TLR values in an adaptive Q system (DFSA) with perfect knowledge of the tag population p at the beginning of each identification cycle. Using this knowledge, the ideal system selects the optimal Q value from Table 1, whose computation is explained in [8]. For each δ considered in Fig. 7, the TLRs obtained by the ideal DFSA are 0, 0.11 and 0.33 respectively. These TLRs are equal to the ones obtained with the optimum static Q values shown in Fig. 7. Therefore, an adaptive procedure, even with perfect knowledge of p , gives no advantage in a mobile RFID system, provided that the physical parameters of the system (v, δ and d) are known in advance.

6. Operative regions

As explained in the preceding section, in a practical RFID application it is desirable, in general, to set a maximum TLR under which the system must operate according to the reliability objectives of the identification process. Let us define the operative region of a tag-moving system as the set of physical parameter values for which the system is able to operate below a maximum allowed TLR. This means that, at any parameter setting within the operative region it is possible to find at least one Q value (optimum Q) providing a TLR below the performance objective. Operative regions can be computed by systematically applying the numerical procedure explained. As an example, Fig. 9 shows the boundaries of the operative regions in terms of tag densities and speeds for several TLR objectives in the reference scenario. The operative regions are given by the area below each boundary curve.

The shape of the boundaries of the operative regions verify that it is the velocity–density product (tag flow) what mainly determines the achievable performance. The points at each boundary have relatively similar tag flows. However, there are differences that are interesting to investigate. Fig. 10 shows the values of the tag flows

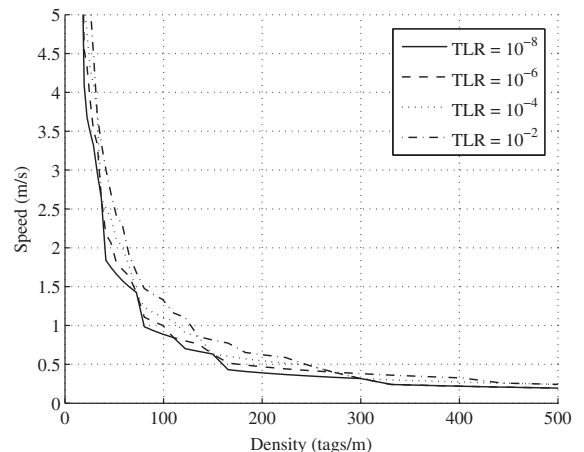


Fig. 9. Boundaries of the speed–density operative regions for several TLR objectives.

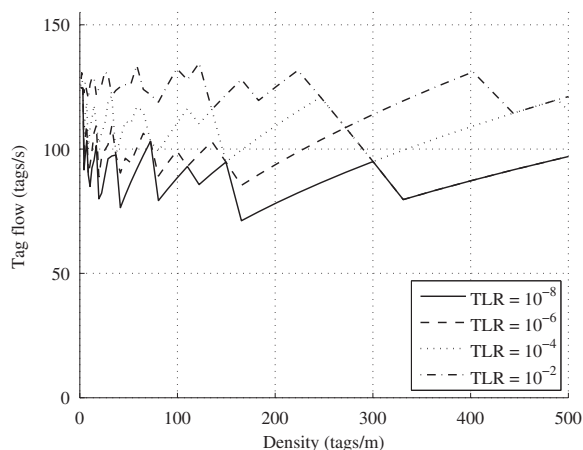


Fig. 10. Incoming tag flow associated to the boundaries of the operative regions.

associated to each operative region depicted in Fig. 9. If both the velocity and the tag density are configurable within a given set of feasible values, the system designer can determine from the curves in Fig. 10 the combination for which the tag flow is maximum for a constant TLR or, in other words, the configuration providing the maximum throughput for a given TLR objective.

7. Conclusions

This paper presents a mathematical model for FSA-based RFID systems with moving tags. This model, validated through simulations, has allowed us to achieve the following goals: first, we have shown that, under certain circumstances, the system considered presents multiple equilibrium points, which was a well-known property of classical slotted ALOHA systems, but had never been reported in a mobile RFID scenario. In consequence, undesirable equilibrium points can be avoided. Second, we have developed a simple procedure to compute the tag loss ratio and therefore to obtain the optimum Q value. Third, we have introduced the concept of operative region, defined as the set of parameter combinations under which the system can operate below a given TLR objective. The operative region, which has practical implications in the design of a real RFID system, can be easily computed by means of our approach.

References

- [1] R. Want, An introduction to RFID technology, *IEEE Pervasive Computing* 5 (1) (2006) 25–33.
- [2] Z.G. Prodanoff, Optimal frame size analysis for framed slotted ALOHA based RFID networks, *Computer Communications* (2009), doi:10.1016/j.comcom.2009.11.007.
- [3] C. Wang, M. Daneshmand, Sohraby, Optimization of tag reading performance in generation-2 RFID protocol, *Computer Communications* 32 (11) (2009) 1346–1352. <http://dx.doi.org/10.1016/j.comcom.2009.02.004>.
- [4] G. Khandelwal, A. Yener, Lee, Kyoungwan, S. Serbetli, ASAP: A MAC Protocol for Dense and Time Constrained RFID Systems, *IEEE International Conference on Communications*, 2006. ICC '06, vol.9, June 2006, pp. 4028–4033.

- [5] Dong-Her Shih, Po-Ling Sun, David C. Yen, Shi-Ming Huang, Taxonomy and survey of RFID anti-collision protocols, *Computer Communications*, 0140-3664 29 (11) (2006) 2150–2166, doi:10.1016/j.comcom.2005.12.011.
- [6] ISO/IEC 18000-6C:2005, Radio-frequency identification for item management-part 6C: parameters for air interface communications at 860 MHz to 960 MHz, January 2005.
- [7] EPCglobal, EPC Radio-frequency Identity Protocols Class-1 Generation-2 UHF RFID Protocol for Communications at 860 MHz–960 MHz, ver 1.0.9, January 2005.
- [8] M.V. Bueno-Delgado, J. Vales-Alonso, On the optimal frame-length configuration on real passive RFID systems, *Journal of Network and Computer Applications*, in Press, ISSN 1084-8045, doi:10.1016/j.jnca.2010.04.022.
- [9] K. Finkenzerler, *RFID handbook: Radio-frequency identification fundamentals and applications*, John Wiley, New York, 2000.
- [10] J. Vales-Alonso, M.V. Bueno-Delgado, E. Egea-López, J.J. Alcaraz, J. García-Haro, Markovian model for Computation of Tags Loss Ratio in Dynamic RFID Systems, 5th European Workshop on RFID Systems and Technologies, Jun. 2009, Bremen, pp. 16–17.
- [11] P. Jankowski-Mihulowicz, W. Kalita, B. Pawlowicz, Problem of dynamic change of tags location in anticollision RFID systems, *Microelectronics Reliability* 48 (6) (2008) 911–918, doi:10.1016/j.microrel.2008.03.006.
- [12] Minhjo Jo, Hee Yong Youn, Si-Ho Cha, Hyunseung Choo, Mobile RFID Tag Detection Influence Factors and Prediction of Tag Detectability, *IEEE Sensors Journal* 9 (2) (2009) 112–119.
- [13] Lei Xie, et. al. Efficient Tag Identification in Mobile RFID Systems, in: *IEEE International Conference INFOCOM 2010*, March 2010, San Diego, CA, pp. 15–19.
- [14] V. Sarangan, M.R. Devarapalli, S. Radhakrishnan, A framework for fast RFID tag reading in static and mobile environments, *Computer Networks* 52 (5) (2008) 1058–1073.
- [15] G. Roussos, V. Kostakos, RFID in pervasive computing: State-of-the-art and outlook, *Pervasive and Mobile Computing* 5 (1) (2009) 110–131. <http://dx.doi.org/10.1016/j.pmcj.2008.11.004>.
- [16] A.B. Carleial, M.E. Hellma, Bistable Behavior of ALOHA-Type System, *IEEE Transactions on Communications* 23 (4) (1975) 401–410.
- [17] Y.-C. Jenq, On the Stability of Slotted ALOHA Systems, *IEEE Transactions on Communications* 28 (11) (1980) 1936–1939.
- [18] L. Kleinrock, *Queueing systems. Volume II: Computer applications*, John Wiley and sons, New York, 1975.
- [19] C. Floerkemeier, Bayesian Transmission Strategy for Framed ALOHA Based RFID Protocols, 2007 IEEE International Conference on RFID, March 2007, pp. 228–235.
- [20] W.-T. Chen, An Accurate Tag Estimate Method for Improving the Performance of an RFID Anticollision Algorithm Based on Dynamic Frame Length ALOHA, *IEEE Transactions on Automation Science and Engineering* 6 (1) (2009) 9–15.
- [21] C. Wang, B. Li, K. Sohraby, M. Daneshmand, Performance analysis of RFID Generation-2 protocol, *IEEE Transactions on Wireless Communications* 8 (5) (2009) 2592–2601.
- [22] J. Vales-Alonso, et. al., Characterization of the Identification Process in RFID Systems, in: Cristina Turcu (Ed.), *Radio Frequency Identification Fundamentals and Applications Bringing Research to Practice*, INTECH, Available from: <http://sciendo.com/articles/show/title/characterization-of-the-identification-process-in-rfid-systems>.
- [23] F. Schoute, Dynamic frame length ALOHA, *IEEE Transactions on Communications* 31 (4) (1983) 565–568.
- [24] R.L. Devaney, *An Introduction to Chaotic Dynamical Systems*, Second ed., Addison-Wesley, 1989.



Juan J. Alcaraz obtained his engineering degree from the Technical University of Valencia (Spain) in 1999. After working for several telecommunication companies he joined the Technical University of Cartagena (Spain) in 2004 where he obtained his Ph.D. in 2007 and currently works as associate professor. He has published several journal papers in the area of wireless networking addressing topics like transport layer performance, access network synchronization, cooperative protocols and scheduling in vehicular communication.



Esteban Egea-López received the Telecommunications Engineering degree in 2000 from the Technical University of Valencia (Spain), the Master Degree in Electronics in 2001, from the University of Gavle (Sweden), and the Ph.D. in Telecommunications in 2006 from the Technical University of Cartagena where he currently works as associate professor. His research interest is focused on ad-hoc and wireless sensor networks.



Joan García-Haro is a professor at the Technical University of Cartagena, Spain. He is author or co-author of more than 60 journal papers mainly in the fields of switching and performance evaluation. From April 2002 to December 2004 he served as EIC of the IEEE Global Communications Newsletter, included in the IEEE Communications Magazine. He is Technical Editor of the same magazine from March 2001. He also holds an Honorable Mention for the IEEE Communications Society Best Tutorial paper Award (1995).



Javier Vales-Alonso is an associate professor at the Department of Information Technologies and Communications in the Technical University of Cartagena (Spain). His main research topics lie in wireless communication areas, mainly in the fields of cellular networks, wireless sensor networks, cognitive radio, vehicular networks, and radio identification. He has been the head of several Spanish national R&D projects related to development of ambient intelligence applications.